Intra-specific variability in deep water extraction between trees growing on a Mediterranean karst

Simon Damien Carrière, Julien Ruffault, Coffi Belmys Cakpo, Albert Olioso, Claude Doussan, Guillaume Simioni, Konstantinos Chalikakis, Nicolas Patris, Hendrik Davi, Nicolas Martin-StPaul

Intra-specific variability in deep water extraction between trees growing on a Mediterranean karst

Simon Damien Carrière[1], Julien Ruffault[2], Coffi Belmys Cakpo[3], Albert Olioso[4], Claude Doussan[4], Guillaume Simioni[2], Konstantinos Chalikakis[4], Nicolas Patris[5], Hendrik Davi[2], Nicolas K. MartinSt-Paul[2].

[1] Sorbonne Université, UPMC, CNRS, EPHE, UMR 7619 METIS, 4 place Jussieu, 75005 Paris, France.

[2] INRAE, URFM, , Domaine Saint Paul, INRAE Centre de recherche PACA, 228 route de l'Aérodrome, CS 40509, Domaine Saint-Paul, Site Agroparc, France.

[3] INRAE, PSH, , Domaine Saint Paul, INRAE Centre de recherche PACA, 228 route de l'Aérodrome, CS 40509, Domaine Saint-Paul, Site Agroparc, France.

[4] INRAE, UMR 1114 EMMAH, Domaine Saint Paul, INRAE Centre de recherche PACA, 228 route de l'Aérodrome, CS 40509, Domaine Saint-Paul, Site Agroparc, France.

[5] Avignon Université, UMR 1114 EMMAH, 301 rue Baruch de Spinoza, BP 21239 84911 Avignon Cedex 9, France.

[6] IRD, Hydroscience Montpellier, 300 Avenue du Professeur Emile Jeanbrau, 34090 Montpellier, France.

Abstract

Plant transpiration is a major component of water fluxes in the critical zone, which needs to be better characterized to improve our ability to understand and model the hydrological cycle. In water-limited ecosystems such as those encountered on karst environments, climate-induced changes in transpiration are expected to be strongly influenced by the ability of the vegetation cover to resist or adapt to drought. However, because of the high heterogeneity of karst environments, the amount of water available for trees can change within a stand, which may lead to significant differences in drought vulnerability resistance between trees of the same species. So far it is not known if soil and subsoil environment influence the magnitude of deep water extraction, at the intra-specific scale. Here, we investigate the variability in deep water extraction for six individual *Quercus ilex* trees growing on a karst substrate in a Mediterranean forest. We combined three approaches: (i) electrical resistivity tomography to determine the variability of soil/subsoil characteristics, (ii) isotope tracing to determine the origin of water transpired by plants, and (iii) predawn and midday leaf water potential (Ψ) to assess the trees' water stress and transpiration regulation. Along the summer season, deep water extraction increased with drought intensity. Deep water use varies between individuals and according to drought intensity. At moderate water stress levels, we found no

significant relationship between the origin of xylem water and soil/subsoil characteristics or individual stress level. However, at the peak of the drought (average predawn $\Psi < -2$ MPa), individuals that had the least total available water in soil/subsoil (0-2m) relied more on deep water and were also subject to less water stress. These results suggest that trees with less favorable soil/subsoil conditions (i.e. low water retention capacity) in the near surface (0-2m) adapt their root systems to exploit deep water reserves more intensively so as to enhance their drought tolerance, while trees with more favorable surface conditions exhibit greater water stress and may be more vulnerable to extreme droughts because of a lower root development in deeper horizons.

Introduction

On one side, a large part of continental precipitation is transpired at the world scale (e.g. Oki et Canae 2006; Maréchal et al. 2009; Fisher et al. 2017). On the other side, the water availability is one of the most important factors driving transpiration, biomass productivity, and plant species distribution in water-limited ecosystems (Rambal et al. 2003; Mathys et al. 2014). Understanding forest response to droughts is a crucial issue under climate change, because of their multiple impacts on ecosystems and society (Kirilenko and Sedjo 2007; Bonan 2008; Taylor et al. 2013). Indeed, ongoing climate change has a strong impact on vegetation (Allen et al. 2010; Anderegg 2015) and changes in vegetation cover have a strong impact on hydrological processes (Scanlon et al. 2005; Nosetto et al. 2012). Deciphering the complex interactions between vegetation cover and hydrological processes is crucial to improve the predictability of climate changes impacts on the hydrological cycle.

The capacity to withdraw water in deep water is a key feature of drought tolerance (Ehleringer et Dawson 1992; Querejeta et al. 2007; Pivavorroff et al. 2016; Brum et al. 2019) that is known to vary among species and contributes, together with other traits, to define the hydrological niches (Brum et al. 2019).

Drought tolerance variability at the intra-specific level, and within a same population, is expected to have a key influence on the evolutionary potential of forests under climate change, and could thereby constitutes an important source of resilience to drought (Bontemps et al. 2017). It could result from of adaptation or plasticity in response to micro local environmental variations.

However there are less data available at intra-specific level, and in particular, the role of deep water exploration for drought tolerance is less clear. Voltas et al. (2015) showed that genetic factors could explain differences in water use on Aleppo pines of various origins grown in common garden test. Barbeta et al. (2015) showed that plasticity could lead to differences in water exploitation for individuals located in a rain exclusion zone and those located in the control zone. Some studies have suggested that micro local variability in soil/subsoil conditions (i.e. water retention capacity, stoniness, soil depth) also explains intra-specific variations of both leaf and tree scale traits (e.g. leaf mass area, foliar $\delta^{13}C$, leaf area index, predawn leaf water potential), (Love et al. 2019; Preisler et al. 2019; Carrière et al. 2020a). More specifically, they suggest that trees with less favorable soil environments have greater acclimation to drought and experience lower water stress and dieback during extreme drought (than trees with higher total available water (TAW)) within soil. But this theory implies two related hypotheses that so far have not been rigorously tested: i) a relationship exists between near-surface soil/subsoil conditions and the ability of individuals to exploit deep water, and ii) this relationship may affect the resistance of individuals to drought.

In this study we aim to assess the relationship between tree water stress, soil/subsoil characteristics, and tree capacity to withdraw deep water, on 6 individual Quercus ilex stems. In particular we explore if soil/subsoil conditions consistently affect tree level water stress and trees' ability to draw water at several depths.

For these purposes, we chose to work in a karst settings where the soil/subsoil conditions are expected to be strongly contrasted between individuals due to the intrinsic heterogeneity of this media (Hartmann et al. 2014). In this type of environment, strong contrasts in soil thickness,

stoniness and water retention capacity can induce a strong variability of soil/subsoil conditions in a few meters, which in turn might influence the develop of root systems for vegetation. We combine three distinct approaches: geophysical, isotopic, and eco-physiological. The first approach, Electrical Resistivity Tomography (ERT), is a non-destructive near-surface geophysical technique used to characterize variability in soil/subsoil conditions (Dahlin 2001; Chalikakis et al. 2011). Unlike classical techniques (e.g. pedologic pits, neutron probe, or Time Domain Reflectometry (TDR) sensors for water), ERT provides an integrated and spatialized (horizontally and vertically) characterization of the near surface at the plot scale. The second approach is water isotope tracing ($\delta^{18}O$), which is used to determine the source of water extracted by plants (Dawson 1993; Querejeta et al. 2007; Nie et al. 2012; Ding et al. 2018). The third approach uses shoot water potential (Ψ), which is widely used to assess plant water stress (Turner 1981). When measured at predawn, transpiration is close to zero, leaf water potential provides an estimate of soil water deficit in the rooting zone. However, when measured during daytime, water potential measurements results from both, soil water deficit and plant hydraulics and transpiration. All datasets used in this study have been described and investigated in previous papers. Carrière et al. (2020a) used ERT to study the variability of foliar traits in response to drought. Carrière et al. (2020b; c) used water isotope combined with predawn and midday leaf water potential to study the variability of deep water use among three species. In this paper, we combine geophysical, isotopic, predawn and midday leaf water potential dataset in an original way to explore the variability of deep water use between individuals of the same species.

Material and Methods

Experimental site

The experimental forest site is located in southern France within the Fontaine-de-Vaucluse observatory (43°56'12''N; 5°27'58''E; 530 m a.s.l.), which is part of the French critical zone observation network (OZCAR - http://www.ozcar-ri.org/; Jourde et al. 2018). The plot, which

measures 150*50 m, is dominated by *Quercus Ilex* L. (85% of the basal area) and an understory (15% of the basal area) dominated by shrubs including *Buxus sempervirens* L., *Juniperus communis* L. and *Juniperus phoenicea* L. (more details can be found in Carrière et al. 2017). The forest was managed as a coppice for charcoal production for centuries before the last clear-cut 90 years ago.

The climate is Mediterranean with dry and hot summers; most rainfall occurs during spring and autumn. Between 2003 and 2015, average annual rainfall was 909 mm and ranged between 407 and 1405 mm. Average annual temperature over the same period was 12.9°C. The soil is a stony rendzina whose thickness is highly variable over the study site. Soil pits excavated along the profile revealed soil depths ranging from 0 to 70 cm. This soil has developed on a karstified calcareous bedrock of Urgonian facies.

Under the experimental plot, a former military bunker has been converted into a scientific laboratory (http://lsbb.eu/presentation/). This underground facility provides an opportunity to sample water flows in the vadose zone at depths of 33 and 256m. Surface-based geophysical exploration showed, with ERT, that the first two meters of the soil/subsoil can store considerable amounts of water (several tens of millimeters) but with high spatial variability at the plot scale (Carrière et al. 2015). Deeper (2 to 90 m) magnetic resonance sounding (MRS) and gravimetry showed seasonal relative variations in water storage that can reach 50% within the vadose zone (Carrière et al. 2016).

Electrical Resistivity Tomography

The ERT dataset used in this study was described by Carrière et al (2015) and then re-used by Carrière et al (2020a) to assess spatial variability of soil/subsoil conditions (i.e. TAW) at the plot level. Additional methodological details about ERT measurements can be found in those two studies. ERT measurements were done using an ABEM Terrameter SAS 4000 device (Dahlin, 2001) with 64 stainless steel electrodes and 2 m spacing along a 126 m transect. The measurement protocol that was used recorded 1140 points. The transect was chosen to align almost perpendicularly to the slope

and geological structures (Carrière et al. 2013) to maximize the variability in soil/subsoil conditions. The inversion quality of the ERT data was evaluated with RMS and Chi², calculated using the raw data and the inverted model (lower-left corner of each cross-section; Figure 1). The resistivity model had a 2 m lateral resolution and a vertical resolution ranging gradually from 0.5 m near the surface to 1.5 m at the base of the cross-section (10 m). A temperature correction was applied on the final model, following Keller et Frischknecht (1966):

$$\rho = \rho_T [1 + \alpha (T - 25)] \quad (1)$$

where ρ (Ω.m) is electrical resistivity at the reference temperature of 25 °C, ρT (Ω.m) is electrical resistivity measured at temperature T (°C), and α is 0.0202. T is underground temperature, logarithmically interpolated between daily mean air temperature aboveground and groundwater temperature at a depth of 30 m.

The Percent Variation in Resistivity (*PVR*) was used to describe the spatial variability of soil/subsoil conditions under each *Quercus Ilex* L. individual. PVR was calculated for each tree as a function of the dry (ρ_{dry}) and wet (ρ_{wet}) resistivity cross-section, as in Clément et al. (2010) and Robert et al. (2012):

$$PVR(\%) = \frac{\rho_{dry} - \rho_{wet}}{\rho_{dry}} * 100 \quad (2)$$

Two ERT measurements were successively carried out in autumn 2011 at an interval of a few days ranging from an extremely dry (i.e. 3 months of drought) to an extremely wet (i.e. after an episode of 230 mm rainfall) status (Figure 1a). The temporal proximity of these measurements and similar meteorological conditions between these two days resulted in very limited variations in air and groundwater temperatures. In Carrière et al. (2020a), we showed that *PVR* between these two dates can be used as a proxy for the total available water (TAW) for vegetation (Figure 1b). The near surface PVR was calculated for each individual by a lateral average within a distance of 2.5 m (corresponding to crown radius) to the stool center and vertically between 0 and 2 m. This thickness corresponds on average to the depth of the massive limestones previously detected by ground

155 penetrating radar (Carrière et al. 2013). We consider that the TAW (0-2m) of each tree is fix
156 parameter in time for a 90 years old stand and that it is its degree of filling that varies over the
157 seasons according to drought level. Therefore, the PVR, which is a proxy of TAW, was measured only
158 once in 2011.

159

160 **Isotopic tracing**

161 **Sampling**

162 The isotopic dataset was published in Carrière et al. (2020c). Field work was conducted on 6 trees at
163 monthly time step between June and August 2015 (06/11/2015 ; 07/06/2015 ; 08/11/2015). On each
164 date, three to four sunny branches with a diameter of 4 to 6 mm were collected from each tree at
165 midday. Phloem and bark were removed to prevent any contamination from phloem sap. The
166 samples were immediately packed in parafilm and placed in sealed vials. These three to four
167 branches were pooled before extraction. A portable cooler was used to transfer the samples to the
168 laboratory where they were stored frozen until water extraction and analyses. Liquid samples of
169 precipitation and drainage water were collected every 1 to 3 weeks. Precipitation was collected
170 through a pluviometer and stored in containers installed in a pit so as to limit temperature variations.
171 Drainage water was collected at 20 cm below the surface using a mini-lysimeter and this water was
172 stored in a separate container (see figure in SI1). These containers were maintained at atmospheric
173 pressure through a capillary to limit exchange between the atmosphere and collected water (IAEA
174 2014), (see figure SI1). The samples were collected on a monthly time step basis and were therefore
175 a mixture of all the water flowed into the cans during the previous month. At this experimental site,
176 the rocky karst soil prevents soil water sampling using auger drilling or porous cups.

177 **Water extraction and isotopic analyses**

Xylem water was extracted from wood by cryogenic vacuum distillation following the protocol of West et al. (2006). The twigs were cut into small pieces and placed in an electrothermal heating and stirring mantle at 90 to 100 °C for 1 hour. Two successive liquid nitrogen traps were used to collect 3 to 5 ml of xylem water. This water was stored in small vials until analyzed.

Deep water and shallow water samples were analyzed using a Los Gatos Isotope Ratio Infrared Spectrometer (IRIS) at Avignon University (LGR DLT-100 liquid water stable analyzer accuracy ±0.2‰ vs V-SMOW for $\delta^{18}O$). The isotopic ratios were expressed as:

$$\delta^{18}O = \left[\left(R_{sample}/R_{standard}\right) - 1\right] \times 1000‰ \quad (3)$$

where $R_{standard}$ and R_{sample} are the light/heavy isotope ratios ($^{16}O/^{18}O$) of the sample and the standard (Vienna Standard Mean Ocean Water (VSMOW)), respectively. Possible spectral perturbations of the IRIS measurements due to organic contaminants in xylem and drainage samples (Martín-Gómez et al. 2015) motivated us to use an Isotope Ratio Mass Spectrometer (IRMS). Xylem and drainage samples were analyzed using the Isoprime IRMS at the LAMA laboratory of HydroSciences Montpellier, using the CO_2 equilibration technique in dual inlet mode, yielding $\delta^{18}O$ results with a ±0.06 ‰ precision. This value was obtained by calculating the standard deviation related to repeated measurements of a standard sample during the analysis of our samples. This precision is reported in Figure 2b and c in the $\delta^{18}O$ error bars.

Leaf water potential

The predawn (Ψ_P) and midday (Ψ_M) leaf water potential dataset was previously published in Carrière et al. (2020a). Both metrics were measured on the 6 individuals chosen for isotope sampling throughout the 2015 summer season using a Scholander pressure bomb. Samples for Ψ_P were collected in the morning, before sunrise. For Ψ_M , samples were collected from sun-exposed branches around midday (2PM GMT), when the sky was not cloudy. For each tree, at least four leaves

were sampled and immediately placed in a plastic bag saturated with water vapor and stored in a portable cooler until measurement (few minutes later). Between two and four leaves were measured to check the consistency between measurements. These multiple measurements were used to determine the error bars shown in Figure 2 b and c. In the results we divided our interpretation into two periods: moderate stress (Ψ_P > -2MPa) and severe stress (Ψ_P < -2MPa) following the work of Lempereur et al (2015).

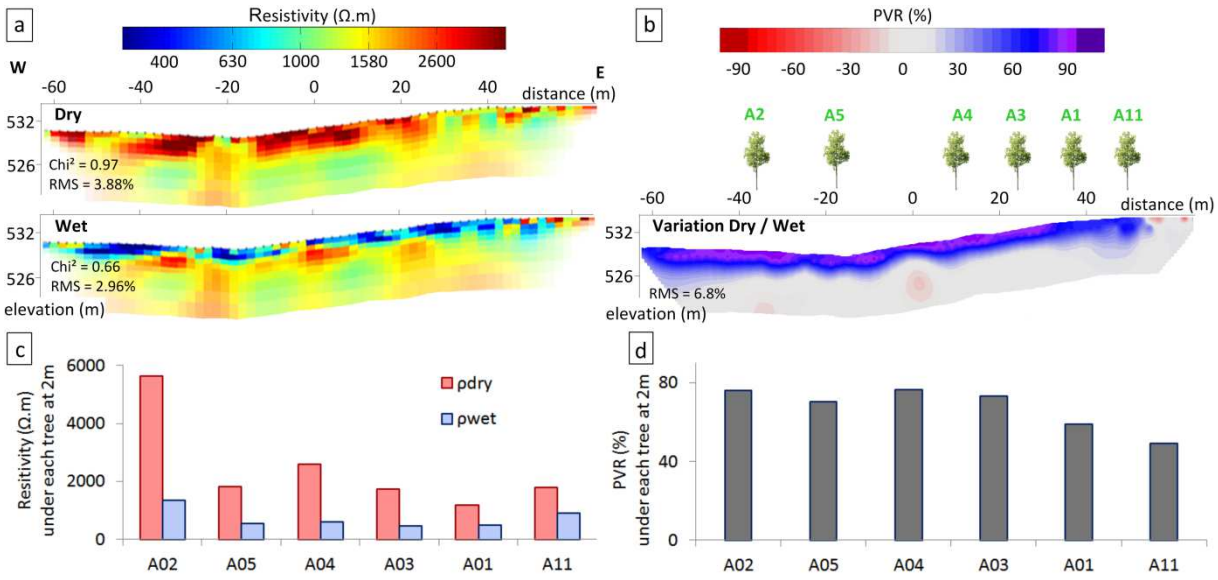

Figure 1: Electrical Resistivity Tomography (ERT) results. (a) ERT models for the "dry" and "wet" dates (respectively before and after a rain event in November 2011), involved in *PVR* computation (equation 2); Gradient arrays, 64 electrodes; ERT model uncertainty, based on current line density, is represented by the color attenuations at the edges and the bottom of the resistivity cross-section. (b) Percent variation in resistivity (*PVR*) between the two resistivity models (dry/wet). (c) Resistivity averaged over 2 m under each tree in dry (ρ_d) and wet period (ρ_w). (d) *PVR* averaged over 2 m under each tree.

Data analysis

We assumed that the isotopic dataset (Carrière et al. 2020c) is affected by an isotopic fractionation in ^{2}H (D-fractionation), therefore we use here only ^{18}O data. D-fractionation is visible in many works

220 (e.g. Brooks et al. 2010; Evaristo et al. 2016; Bowling et al. 2017; Evaristo et al. 2017; Geris et al.
221 2017; Vargas et al. 2017). The causes of this fractionation are still poorly understood (Barbeta et al.
222 2019). Early studies have assumed that D-fractionation is related to the mode of water absorption by
223 roots (Sternberg and Swart 1987; Lin and Sternberg 1993; Ellsworth and Williams 2007). Barbeta et
224 al. (2020) suggest that D-fractionation is rather related to the heterogeneity of the water signal in soil
225 pores and plant tissues. Ellsworth et al. (2007) and Barbeta et al. (2020) agree that fractionation is
226 much stronger in ^{2}H than in ^{18}O and that ^{18}O provides more satisfactory analysis.

227 Therefore, considering only one valid tracer (^{18}O), we had to simplify our analysis into only two
228 potential pools of plant supply: i) the shallow pool or ii) the deep pool (Fig. SI2). Rain and drainage
229 water were analyzed separately, but the two datasets are similar during summer. We arithmetically
230 averaged the two values to represent the "shallow water" signal in Figure 2b and c. Deep water was
231 collected at two seepage points (named "Point C" and "Point D") within the LSBB tunnel
232 (http://lsbb.eu/presentation/) under the experimental site. These two points were arithmetically
233 averaged to represent the "deep water" signal of the karst vadose zone in Figure 2b and c. We
234 assume that this "deep water" signal corresponds to water contained within rock, as described by
235 Bowling et al. (2017) and Geris et al. (2017).

236 The analysis presented in this paper is based on two previously published dataset (Carrière et al.
237 2020a, b). Combining both datasets, only six trees were prospected by geophysics and were
238 monitored in $\delta^{18}O$ and Ψ along the summer period 2015. The logistical difficulty for data acquisition
239 explains this small sample. We therefore evaluated the correlation between the parameters using
240 the Pearson correlation, but also the Spearman correlation which is recommended for the analysis of
241 small samples.

242

243 **Results and interpretation**

244 **Spatial variability in soil/subsoil properties at tree scale assessed with ERT**

We observed wide variations in resistivity both within and between the driest and wettest profiles measured in 2011 (Figure 1a), from less than 300 Ω.m in wet conditions to more than 2500 Ω.m in dry conditions. We note that the resistivity signal was more stable between the two profiles in deep (> 2 m) than in shallow (<2m) layers (Fig. 1a), which caused *PVR* to be smaller in deeper layers (Figure 1b).

PVR patterns showed consistent signals with field soil observations and total available water (TAW) measurements. For instance, the cross section reveals a low *PVR* to the right of tree A11, which is consistent with field observations showing limestone rock outcrops in this area (see SI3). We also observed a consistent trend between *PVR* and TAW estimated through pedologic pits (see SI4). This was discussed in Carrière et al. (2020a) and provides further evidence that *PVR* is well suited to quantifying TAW relatively.

In the following, *PVR* (0 - 2 m) is used as a proxy for TAW. As an example, *PVR* values indicate that tree A4 has a higher TAW than A11. We will examine in the following results whether these trees have contrasting $\delta^{18}O$ and Ψ_M signals. Note that the *PVR* is a constant value for each tree, unlike $\delta^{18}O$ and Ψ_M, which vary throughout the season.

Individual drought adaptation strategies

Tree water deficits increased during the 2015 summer season, as shown by the clear decrease in average Ψ_P and Ψ_M leaf water potentials from June to August 2015 (Figure 2a). Concurrently, the difference between Ψ_P and Ψ_M tended to decrease during the summer season, suggesting that trees regulate their transpiration as drought increases. At the individual scale (Figure 2b), we observed that tree A11 was systematically less stressed than tree A4. Moreover, the range of Ψ_P among individuals increased with drought.

During moderate water deficit (Ψ_P > -2 MPa, June and July), there was no clear relationship between Ψ_P and $\delta^{18}O$ of the xylem (Figure 2b ; p-value > 0.4). By contrast, at the peak of the drought (August 2015), we observed a significant negative relationship between Ψ_P and $\delta^{18}O$ of the xylem (p-value

< 0.001). This implies that the least stressed trees (with the highest water potentials) had an isotopic signal closer to the isotopic signal of groundwater while the more stressed trees (with the lowest water potential) had an isotopic signal closer to shallow water. There was no relationship between Ψ_M and $\delta^{18}O$ at any period in 2015 (Fig. SI5). This is probably due to the fact that Ψ_M is dependent on soil water status but also on additional environmental (light and vapor pressure deficit) and biological factors including plant hydraulic conductance, tree transpiration) that blurred its relations with soil related metrics.

Similarly, no significant relationship was observed between the isotopic signal and *PVR* among individuals when stress is moderate, but a significant relationship (p-value < 0.05) was observed in drier conditions (Fig. 2c). Trees with a low *PVR* between 0 and 2 m (i.e. low TAW) had a $\delta^{18}O$ signal closer to groundwater while trees with a high *PVR* (0-2 m) had an isotopic signal closer to shallow water.

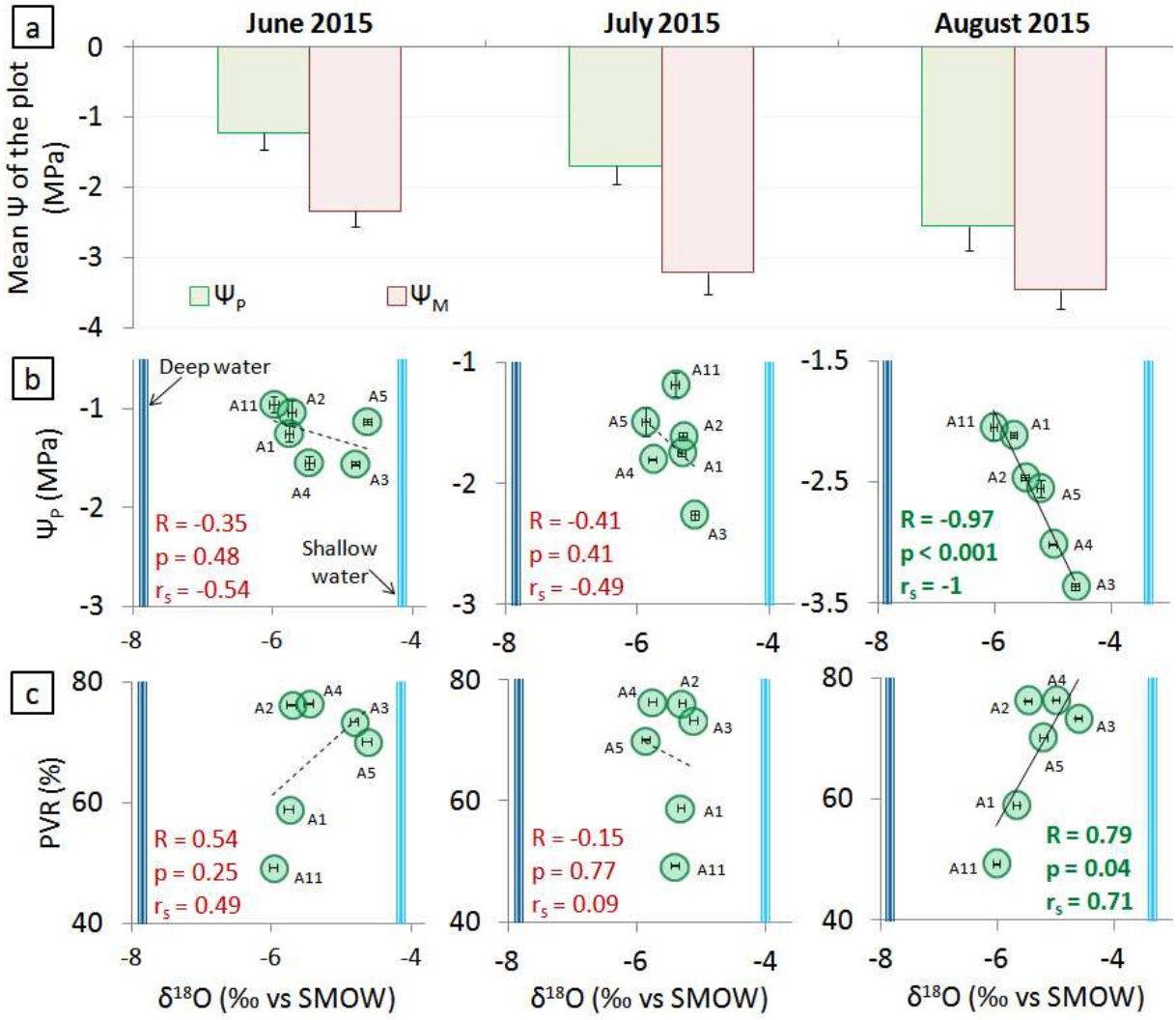

Figure 2 : a) Mean and standard deviation values for leaf water potential of the stand at predawn (Ψ_P) and midday (Ψ_M) for the months of June, July, and August 2015; b) Relationship between Ψ_P and the xylem isotope signal ($\delta^{18}O$) for each individual (each point is a tree), the dark blue and light blue vertical bars represent the groundwater and shallow water isotope signals, respectively. *R* is Pearson correlation, *p* is p-value, and r_s is Spearman correlation; c) Relationship between *PVR* and xylem $\delta^{18}O$ during the summer 2015.

Discussion and perspectives

The variability in drought response at the intra-specific level within a stand can be a key feature of stand resilience to climate change (Albert et al. 2012). However, the belowground processes involved

293 in such variability remain poorly known. In Carrière et al. (2020a) we showed that trees with low near
294 surface TAW (low PVR) experienced higher stomatal control and lower water stress during drought
295 peak compared to trees with higher TAW, which experienced higher water stress and a higher
296 defoliation rates following extreme drought (see SI6). In this study, for the first time, we analyzed
297 together ERT, water potential measurements, and isotopic data to further show that there is a link
298 between near-surface TAW, water status, and tree ability to exploit deep water.

299 We found a negative correlation between tree $\delta^{18}O$ and Ψ_P of individuals at the drought peak in
300 August 2015, indicating that the individuals experiencing higher water stress relied proportionately
301 less on deep water sources than the others. This drought dependence of the xylem isotope signal had
302 already been demonstrated across different species (Flanagan et al. 1992; Jackson et al. 1995; Brum
303 et al. 2019) or in the course of drought for a single species (Barbetta et al. 2015; Carrière et al.
304 2020b). However, to our knowledge, this is the first time that such mechanism is reported at the
305 intra-specific level. Furthermore, we show that trees with low TAW (0-2 m) rely proportionally more
306 on deep water during drought peaks. A likely explanation for this pattern is that trees with low TAW
307 would have developed deeper root into the karst vadoze zone on which they could rely when
308 drought becomes critical (Figure 3). This hypothesis would explain why we observed an isotopic
309 signal closer to deep water and a lower vulnerability to intense droughts for trees with higher TAW. A
310 schematic interpretation of our results is presented in Figure 3.

311 Drought resistance variability among individuals of the same species is rarely considered in ecological
312 studies despite its role in forest structure and outcomes under ongoing climate change. Here we
313 show strong variability between individuals that can be partially explained by underground factors
314 (TAW, ability of trees to extract deep water). This implies that stand resistance to drought may be
315 more heterogeneous than is currently predicted by current ecosystem models. For instance, our
316 conclusions may explain the results of several studies showing that tree dieback following drought

317 occurs more frequently in areas where trees benefit from well-developed soils (Nourtier et al 2014;
318 Preisler et al. 2019; Carrière et al 2020a).

319 Further experiments should be carried out on a larger scale and on multiple species to generalize our
320 results, and to evaluate if inter and intra-specific differences overlap. We already obtained
321 encouraging results by enriching the Ψ_P and $\delta^{18}O$ relationship (Figure 2b) with data observed in
322 August 2015 on beech and silver fir trees at a nearby site located at slightly higher altitude (Figure
323 SI7). It would also be interesting to assess if deep water extraction scale with root biomass in
324 factures, that can be estimated with non-invasive method (Mary et al. 2019).

325 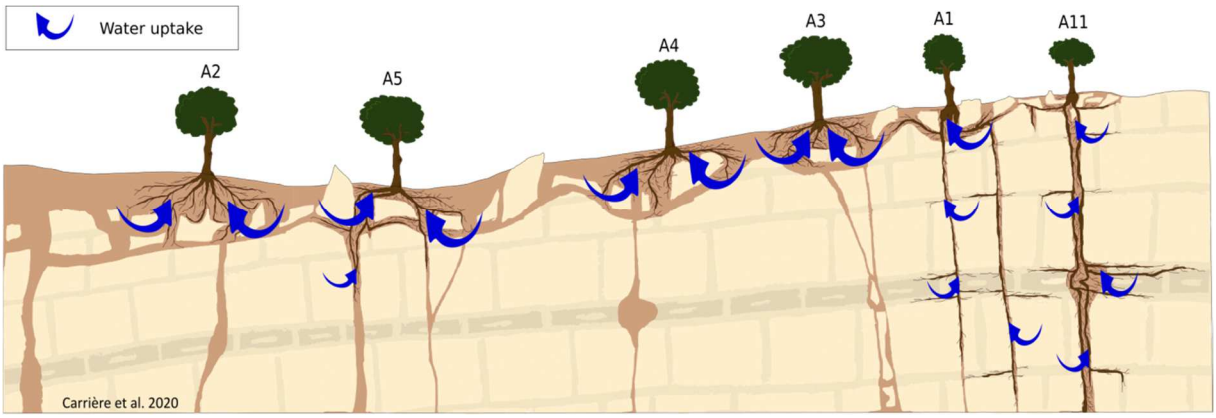

326 Figure 3: Schematic interpretation of tree root implantation as a function of their soil/subsoil
327 condition identified by geophysics (Figure 1b), and their response to drought (Ψ_P and $\delta^{18}O$). The
328 representation of the crown size of each tree is proportional to its individual leaf area, which is also
329 related to soil/subsoil conditions (Carrière et al. 2020a).

330

331 **Conclusions**

332 The combination of geophysics, isotopes, and foliar water potentials open fruitful research avenues
333 to clarify plant-water relationships and tree response to drought. Significant differences in water
334 stress were observed between the trees of the same species growing on a Mediterranean karst. Our
335 analysis clearly suggest that such differences are due to karst heterogeneity, which imposes

contrasted soil/subsoil conditions (i.e. TAW) between individual. We have shown that trees with the least favorable near-surface (0-2m) soil/subsoil conditions proportionately extract more deep water in periods of severe stress. We hypothesis that deep water extraction can be considered as an adaptation mechanism to recurrent water deficit. It is crucial to better understand these adaptation mechanisms in order to better anticipate the impact of changes in vegetation cover on hydrological processes.

Acknowledgments

This work benefited from fruitful discussions within the KARST observatory network (SNO KARST) initiative from the INSU/CNRS and OZCAR, which aims to strengthen knowledge sharing and promote cross-disciplinary research on karst systems at the national scale. We acknowledge H+ network of hydrogeological research sites for co-funding a part of this research. INRA supported this research in the framework of the metaprogramme Adaptation of Agriculture and Forests to Climate Change (ACCAF) of the French National Institute for Agricultural Research (INRA).

References

Albert, C.H., de Bello, F., Boulangeat, I., Pellet, G., Lavorel, S., Thuiller, W., 2012. On the importance of intraspecific variability for the quantification of functional diversity. Oikos 121, 116–126.

Allen, C.D., Macalady, A.K., Chenchouni, H., Bachelet, D., McDowell, N., Vennetier, M., Kitzberger, T., Rigling, A., Breshears, D.D., Hogg, E.T., 2010. A global overview of drought and heat-induced tree mortality reveals emerging climate change risks for forests. Forest ecology and management 259, 660–684.

359 Anderegg, W.R., Konings, A.G., Trugman, A.T., Yu, K., Bowling, D.R., Gabbitas, R., Karp, D.S., Pacala, S.,
360 Sperry, J.S., Sulman, B.N., 2018. Hydraulic diversity of forests regulates ecosystem resilience during
361 drought. Nature 561, 538–541.

362 Barbeta, A., Gimeno, T.E., Clavé, L., Fréjaville, B., Jones, S.P., Delvigne, C., Wingate, L., Ogée, J., 2020.
363 An explanation for the isotopic offset between soil and stem water in a temperate tree species. New
364 Phytologist.

365 Barbeta, A., Jones, S.P., Clavé, L., Wingate, L., Gimeno, T.E., Fréjaville, B., Wohl, S., Ogée, J., 2019.
366 Unexplained hydrogen isotope offsets complicate the identification and quantification of tree water
367 sources in a riparian forest. Hydrology and Earth System Sciences 23, 2129–2146.
368 https://doi.org/10.5194/hess-23-2129-2019

369 Barbeta, A., Mejía-Chang, M., Ogaya, R., Voltas, J., Dawson, T.E., Peñuelas, J., 2015. The combined
370 effects of a long-term experimental drought and an extreme drought on the use of plant-water
371 sources in a Mediterranean forest. Global Change Biology 21, 1213–1225.
372 https://doi.org/10.1111/gcb.12785

373 Bonan, G.B., 2008. Forests and climate change: forcings, feedbacks, and the climate benefits of forests.
374 science 320, 1444–1449.

375 Bontemps, A., Davi, H., Lefèvre, F., Rozenberg, P., Oddou-Muratorio, S., 2017. How do functional traits
376 syndromes covary with growth and reproductive performance in a water-stressed population of
377 Fagus sylvatica? Oikos 126, 1472–1483.

378 Bowling, D.R., Schulze, E.S., Hall, S.J., 2017. Revisiting streamside trees that do not use stream water:
379 can the two water worlds hypothesis and snowpack isotopic effects explain a missing water source?
380 Ecohydrology 10, e1771.

381 Brooks, J.R., Barnard, H.R., Coulombe, R., McDonnell, J.J., 2010. Ecohydrologic separation of water
382 between trees and streams in a Mediterranean climate. Nature Geoscience 3, 100.

383 Brum, M., Vadeboncoeur, M.A., Ivanov, V., Asbjornsen, H., Saleska, S., Alves, L.F., Penha, D., Dias, J.D.,
384 Aragão, L.E., Barros, F., 2019. Hydrological niche segregation defines forest structure and drought
385 tolerance strategies in a seasonal Amazon forest. Journal of Ecology 107, 318–333.

386 Carrière, S.D., Ruffault, J., Pimont, F., Doussan, C., Simioni, G., Chalikakis, K., Limousin, J.-M., Scotti, I.,
387 Courdier, F., Cakpo, C.-B., 2020a. Impact of local soil and subsoil conditions on inter-individual
388 variations in tree responses to drought: insights from Electrical Resistivity Tomography. Science of
389 the Total Environment 698, 134247.

390 Carrière, S.D., Martin-StPaul, N.K., Cakpo, C.B., Patris, N., Gillon, M., Chalikakis, K., Doussan, C., Olioso,
391 A., Babic, M., Jouineau, A., Simioni, G., Davi, H., 2020b. The role of deep vadose zone water in tree
392 transpiration during drought periods in karst settings–Insights from isotopic tracing and leaf water
393 potential. Science of the Total Environment 699, 134332.

394 Carrière, S.D., Martin-StPaul, N.K., Cakpo, C.B., Patris, N., Gillon, M., Chalikakis, K., Doussan, C., Olioso,
395 A., Babic, M., Jouineau, A., 2020c. Tree xylem water isotope analysis by Isotope Ratio Mass
396 Spectrometry and Laser Spectrometry: a dataset to explore tree response to drought. Data in Brief
397 105349.

398 Carrière, S.D., Danquigny, C., Davi, H., Chalikakis, K., Ollivier, C., Martin-StPaul, N.K., Emblanch, C.,
399 2017. Process-Based Vegetation Models Improve Karst Recharge Simulation Under Mediterranean
400 Forest, in: EuroKarst 2016, Neuchâtel. Springer, pp. 109–116.

401 Carrière, S.D., Chalikakis, K., Danquigny, C., Davi, H., Mazzilli, N., Ollivier, C., Emblanch, C., 2016. The
402 role of porous matrix in water flow regulation within a karst unsaturated zone: an integrated
403 hydrogeophysical approach. Hydrogeology Journal 24, 1905–1918.

404 Carrière, S.D., Chalikakis, K., Danquigny, C., Clément, R., Emblanch, C., 2015. Feasibility and Limits of
405 Electrical Resistivity Tomography to Monitor Water Infiltration Through Karst Medium During a Rainy
406 Event, in: Andreo, B., Carrasco, F., Durán, J.J., Jiménez, P., LaMoreaux, J.W. (Eds.), Hydrogeological

407 and Environmental Investigations in Karst Systems. Springer Berlin Heidelberg, pp. 45–55.
408 https://doi.org/10.1007/978-3-642-17435-3_6

409 Carrière, S.D., Chalikakis, K., Sénéchal, G., Danquigny, C., Emblanch, C., 2013. Combining Electrical
410 Resistivity Tomography and Ground Penetrating Radar to study geological structuring of karst
411 Unsaturated Zone. Journal of Applied Geophysics 94, 31–41.
412 https://doi.org/10.1016/j.jappgeo.2013.03.014

413 Chalikakis, K., Plagnes, V., Guerin, R., Valois, R., Bosch, F.P., 2011. Contribution of geophysical methods
414 to karst-system exploration: an overview. Hydrogeol. J. 19, 1169–1180.
415 https://doi.org/10.1007/s10040-011-0746-x

416 Chitra-Tarak, R., Ruiz, L., Dattaraja, H.S., Kumar, M.M., Riotte, J., Suresh, H.S., McMahon, S.M.,
417 Sukumar, R., 2018. The roots of the drought: Hydrology and water uptake strategies mediate
418 forest-wide demographic response to precipitation. Journal of Ecology 106, 1495–1507.

419 Clément, R., Descloitres, M., Günther, T., Oxarango, L., Morra, C., Laurent, J.P., Gourc, J.P., 2010.
420 Improvement of electrical resistivity tomography for leachate injection monitoring. Waste
421 Management 30, 452–464. https://doi.org/10.1016/j.wasman.2009.10.002

422 Dahlin, T., 2001. The development of DC resistivity imaging techniques. Computers & Geosciences 27,
423 1019–1029. https://doi.org/10.1016/s0098-3004(00)00160-6

424 Dawson, T.E., 1993. Hydraulic lift and water use by plants: implications for water balance, performance
425 and plant-plant interactions. Oecologia 95, 565–574.

426 Ding, Y., Nie, Y., Schwinning, S., Chen, H., Yang, J., Zhang, W., Wang, K., 2018. A novel approach for
427 estimating groundwater use by plants in rock-dominated habitats. Journal of hydrology 565, 760–
428 769.

429 Ellsworth, P.Z., Williams, D.G., 2007. Hydrogen isotope fractionation during water uptake by woody
430 xerophytes. Plant and Soil 291, 93–107.

Evaristo, J., McDonnell, J.J., Clemens, J., 2017. Plant source water apportionment using stable isotopes: A comparison of simple linear, two-compartment mixing model approaches. Hydrological Processes 31, 3750–3758. https://doi.org/10.1002/hyp.11233

Evaristo, J., McDonnell, J.J., Scholl, M.A., Bruijnzeel, L.A., Chun, K.P., 2016. Insights into plant water uptake from xylem-water isotope measurements in two tropical catchments with contrasting moisture conditions. Hydrological Processes 30, 3210–3227.

Fisher, J.B., Melton, F., Middleton, E., Hain, C., Anderson, M., Allen, R., McCabe, M.F., Hook, S., Baldocchi, D., Townsend, P.A., 2017. The future of evapotranspiration: Global requirements for ecosystem functioning, carbon and climate feedbacks, agricultural management, and water resources. Water Resources Research 53, 2618–2626.

Flanagan, L., Ehleringer, J., Marshall, J., 1992. Differential uptake of summer precipitation among co-occurring trees and shrubs in a pinyon-juniper woodland. Plant, Cell & Environment 15, 831–836.

Geris, J., Tetzlaff, D., McDonnell, J.J., Soulsby, C., 2017. Spatial and temporal patterns of soil water storage and vegetation water use in humid northern catchments. Science of the Total Environment 595, 486–493.

Hartmann, A., Goldscheider, N., Wagener, T., Lange, J., Weiler, M., 2014. Karst water resources in a changing world: Review of hydrological modeling approaches. Reviews of Geophysics 52, 218–242. https://doi.org/10.1002/2013RG000443

IAEA, 2014. IAEA/GNIP precipitation sampling guide [WWW Document]. URL http://www-naweb.iaea.org/napc/ih/documents/other/gnip_manual_v2.02_en_hq.pdf (accessed 1.23.19).

Jackson, P., Cavelier, J., Goldstein, G., Meinzer, F., Holbrook, N., 1995. Partitioning of water resources among plants of a lowland tropical forest. Oecologia 101, 197–203.

453 Jourde, H., Massei, N., Mazzilli, N., Binet, S., Batiot-Guilhe, C., Labat, D., Steinmann, M., Bailly-Comte,
454 V., Seidel, J., Arfib, B., 2018. SNO KARST: A French network of observatories for the multidisciplinary
455 study of critical zone processes in karst watersheds and aquifers. Vadose Zone Journal 17.

456 Keller, G.V., Frischknecht, F.C., 1966. Electrical methods in geophysical prospecting. International
457 Series of Monographs in Electromagnetic Waves 10.

458 Kirilenko, A.P., Sedjo, R.A., 2007. Climate change impacts on forestry. Proceedings of the National
459 Academy of Sciences 104, 19697–19702.

460 Knighton, J., Souter-Kline, V., Volkman, T., Troch, P.A., Kim, M., Harman, C., Morris, C., Buchanan, B.,
461 Walter, M.T., 2019. Seasonal and topographic variations in ecohydrological separation within a small,
462 temperate, snow-influenced catchment. Water Resources Research 55, 6417–6435.

463 Lempereur, M., Martin-StPaul, N.K., Damesin, C., Joffre, R., Ourcival, J., Rocheteau, A., Rambal, S.,
464 2015. Growth duration is a better predictor of stem increment than carbon supply in a
465 Mediterranean oak forest: implications for assessing forest productivity under climate change. New
466 Phytologist 207, 579–590.

467 Lin, G., da Sternberg, L.S.L., 1993. Hydrogen isotopic fractionation by plant roots during water uptake
468 in coastal wetland plants, in: Stable Isotopes and Plant Carbon-Water Relations. Elsevier, pp. 497–
469 510.

470 Love, D., Venturas, M., Sperry, J., Brooks, P., Pettit, J.L., Wang, Y., Anderegg, W., Tai, X., Mackay, D.,
471 2019. Dependence of aspen stands on a subsurface water subsidy: Implications for climate change
472 impacts. Water Resources Research 55, 1833–1848.

473 Maréchal, J.-C., Varma, M.R., Riotte, J., Vouillamoz, J.-M., Kumar, M.M., Ruiz, L., Sekhar, M., Braun, J.-
474 J., 2009. Indirect and direct recharges in a tropical forested watershed: Mule Hole, India. Journal of
475 Hydrology 364, 272–284.

476 Martín-Gómez, P., Barbeta, A., Voltas, J., Peñuelas, J., Dennis, K., Palacio, S., Dawson, T.E., Ferrio, J.P.,
477 2015. Isotope-ratio infrared spectroscopy: a reliable tool for the investigation of plant-water
478 sources? New Phytologist 207, 914–927.

479 Mary, B., Vanella, D., Consoli, S., Cassiani, G., 2019. Assessing the extent of citrus trees root apparatus
480 under deficit irrigation via multi-method geo-electrical imaging. Scientific reports 9, 9913.

481 Mathys, A., Coops, N.C., Waring, R.H., 2014. Soil water availability effects on the distribution of 20 tree
482 species in western North America. Forest ecology and management 313, 144–152.

483 Nie, Y., Chen, H., Wang, K., Yang, J., 2012. Water source utilization by woody plants growing on
484 dolomite outcrops and nearby soils during dry seasons in karst region of Southwest China. Journal of
485 Hydrology 420, 264–274.

486 Nourtier, M., Chanzy, A., Cailleret, M., Yingge, X., Huc, R., Davi, H., 2014. Transpiration of silver Fir
487 (Abies alba mill.) during and after drought in relation to soil properties in a Mediterranean mountain
488 area. Annals of forest science 71, 683–695.

489 Oki, T., Kanae, S., 2006. Global hydrological cycles and world water resources. science 313, 1068–1072.

490 Preisler, Y., Tatarinov, F., Grünzweig, J.M., Bert, D., Ogée, J., Wingate, L., Rotenberg, E., Rohatyn, S.,
491 Her, N., Moshe, I., 2019. Mortality versus survival in drought-affected Aleppo pine forest depends on
492 the extent of rock cover and soil stoniness. Functional Ecology 33, 901–912.

493 Querejeta, J.I., Estrada-Medina, H., Allen, M.F., Jiménez-Osornio, J.J., 2007. Water source partitioning
494 among trees growing on shallow karst soils in a seasonally dry tropical climate. Oecologia 152, 26–36.

495 Rambal, S., Ourcival, J.-M., Joffre, R., Mouillot, F., Nouvellon, Y., Reichstein, M., Rocheteau, A., 2003.
496 Drought controls over conductance and assimilation of a Mediterranean evergreen ecosystem:
497 scaling from leaf to canopy. Global Change Biology 9, 1813–1824. https://doi.org/10.1111/j.1365-
498 2486.2003.00687.x

499 Robert, T., Caterina, D., Deceuster, J., Kaufmann, O., Nguyen, F., 2012. A salt tracer test monitored
500 with surface ERT to detect preferential flow and transport paths in fractured/karstified limestones.
501 Geophysics 77, B55–B67. https://doi.org/10.1190/geo2011-0313.1

502 Scanlon, B.R., Reedy, R.C., Stonestrom, D.A., Prudic, D.E., Dennehy, K.F., 2005. Impact of land use and
503 land cover change on groundwater recharge and quality in the southwestern US. Global Change
504 Biology 11, 1577–1593. https://doi.org/10.1111/j.1365-2486.2005.01026.x

505 Silvertown, J., Araya, Y., Gowing, D., 2015. Hydrological niches in terrestrial plant communities: a
506 review. Journal of Ecology 103, 93–108.

507 Sternberg, L. da S.L., Swart, P.K., 1987. Utilization of freshwater and ocean water by coastal plants of
508 southern Florida. Ecology 68, 1898–1905.

509 Turner, N.C., 1981. Techniques and experimental approaches for the measurement of plant water
510 status. Plant and soil 58, 339–366.

511 Vargas, A.I., Schaffer, B., Yuhong, L., Sternberg, L. da S.L., 2017. Testing plant use of mobile vs
512 immobile soil water sources using stable isotope experiments. New Phytologist 215, 582–594.

513 West, A.G., Patrickson, S.J., Ehleringer, J.R., 2006. Water extraction times for plant and soil materials
514 used in stable isotope analysis. Rapid Communications in Mass Spectrometry 20, 1317–1321.
515 https://doi.org/10.1002/rcm.2456

516 Wortemann, R., Herbette, S., Barigah, T.S., Fumanal, B., Alia, R., Ducousso, A., Gomory, D., Roeckel-
517 Drevet, P., Cochard, H., 2011. Genotypic variability and phenotypic plasticity of cavitation resistance
518 in Fagus sylvatica L. across Europe. Tree physiology 31, 1175–1182.

519

520

521